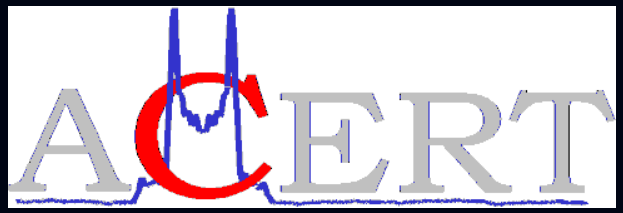

ACERT 2013 Workshop
"PDS & Protein" June 12 – 14, 2013

Introduction & PDS ESR at ACERT

Jack H. Freed, Director
ACERT

National Biomedical Center for Advanced ESR Technology

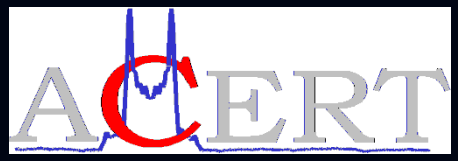

- **ACERT's main objective is to encourage & facilitate biomedical & biophysical research by modern ESR methods.**

- **ACERT represents a unique blend of instrumentation & experimental & theoretical capabilities that address modern biomedical & biophysical research.**

ESR Technologies at ACERT

- **Pulsed Dipolar Spectroscopies**
  - Accurate Distances in Biomolecules
  - Protein Structure & Function
  - New Pulse Dipolar Methods
- **Two-Dimensional Fourier Transform ESR: 2D-ELDOR**
  - Dynamic Structure in Membranes & Proteins
  - Time Resolved Studies of Functional Dynamics in Biosystems
- **High Frequency Quasi-Optical ESR**
  - New Quasi-Optical Technologies
  - Multi-Frequency Studies of Complex Dynamics in Proteins & Membranes
  - Extension of Pulsed 2D-ELDOR to High Frequencies
- **ESR Microscopy**
  - New Technology For Micro-Imaging of Biosamples Including Tissues & Cells

Center Resources: ESR Spectrometers*

1. **Bruker GmbH, ELEXYS E500 9 GHz spectrometer** For General & Service Work.

2. **ACERT 9/17 PDS & 2D-FT-ESR (4kW) pulse spectrometer.**

3. **ACERT 8-18 GHz 2D-FT-ESR & PDS (8kW, X Band), (4kW, Ku Band) pulse spectrometer** (newly operating).

4. **ACERT 35 GHz PDS-ESR (1kW) pulse & CW spectrometer** (newly operating).

5. **ACERT 170/240 GHz quasi-optical, reflection-induction mode CW spectrometer.**

6. **ACERT 95 GHz quasi-optical induction-mode CW & high power (1kW) pulse spectrometer.**

7. **ACERT 9/16 GHz pulse ESR microscope.**

*These spectrometers have all been constructed &/or developed at ACERT (except for Bruker).

Pulse Dipolar Spectroscopies

The Virtues of PDS

a) Many biological objects can be studied: soluble & membrane proteins & protein complexes, RNA, DNA, peptides, polymers.

b) A variety of sample types possible: solutions, liposomes, micelles, bicelles, multi-bilayer vesicles, biological membranes.

c) A variety of sample morphologies possible: it can be uniform, ordered, heterogeneous, etc.

d) Broad range of concentrations from micromolar to tens of millimolar is amenable & very small amounts of biomolecule of interest are sufficient.

The Virtues of PDS

continued...

e) Distances yielded by PDS span wide range of 10-90Å & they are fairly accurate. Therefore, a relatively small number of them is sufficient to reveal structures. A single distance can address important structural & functional details.

f) Conformational flexibility is efficiently dealt with. Several methods for data analysis, in particular based on Tikhonov reconstruction greatly simplify the task of extracting average distances & distance distributions from experimental data.

A Pair Of Electron Spins S_1 & S_2 Coupled Via The Electron Spin Dipole–dipole Interaction

$$a = \omega_d(1-3\cos^2\theta)$$

Spins Along B_0

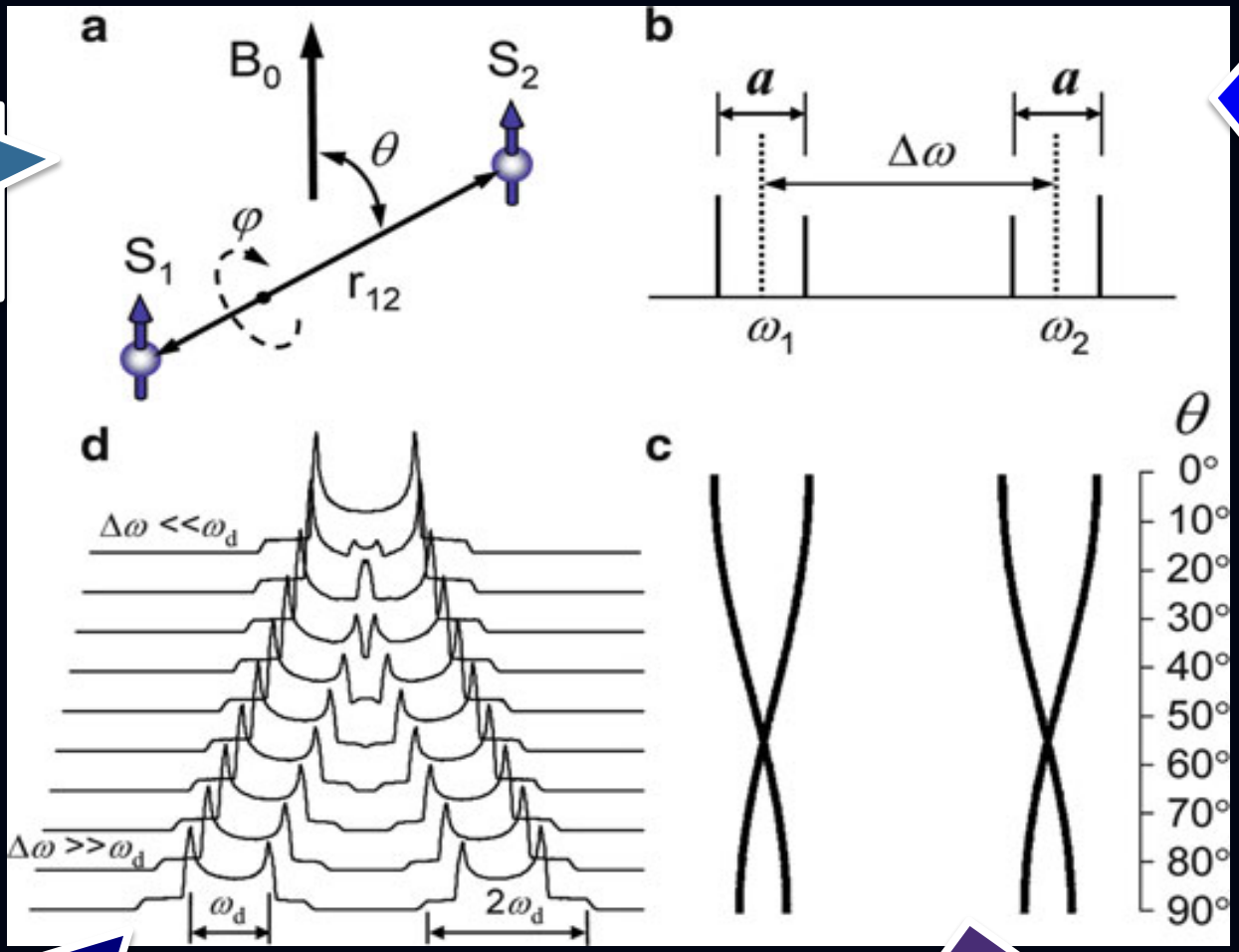

Dipolar coupling splits the spectrum of 2 electron spins into doublets

Strong coupling (Upper) to weak coupling (lower)

Angular dependence is shown as Road Map

Protein Structure Determination Using Long-Distance Constraints from Double-Quantum Coherence(DQC) ESR: T4–Lysozyme (with P. Borbat* & H.S. Mchaourab , JACS 124, 5304 (2002))

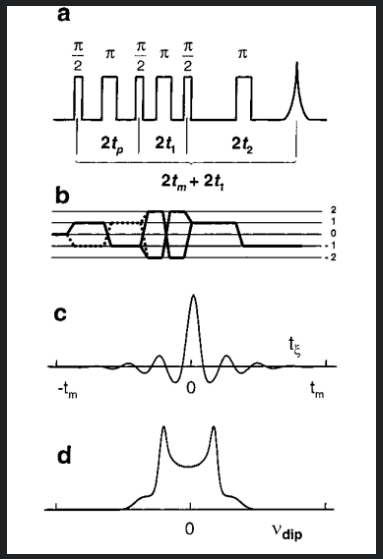

DQC-ESR Pulse Sequence
π/2 pulses = 3.2 ns
π pulses = 6.4 ns

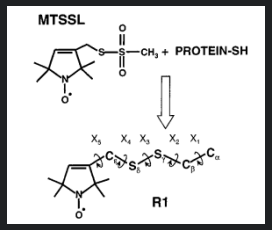

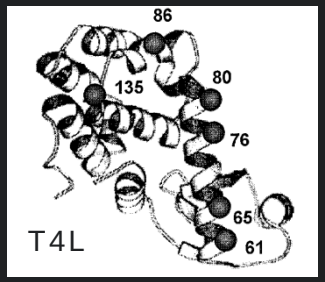

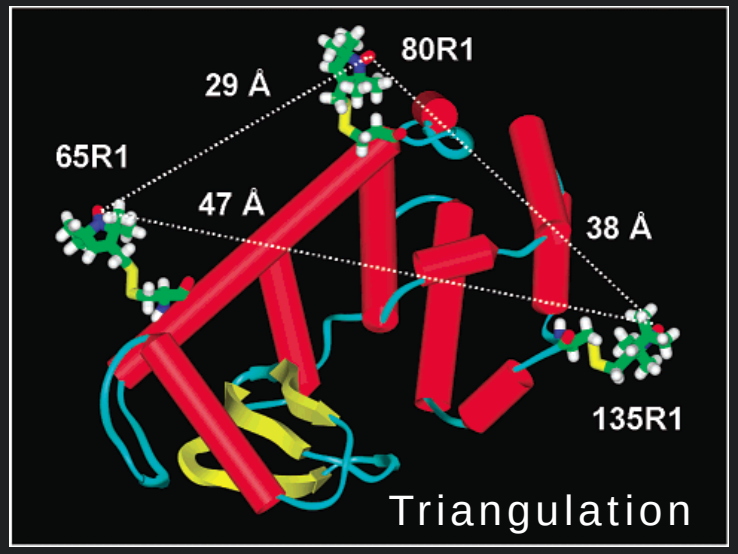

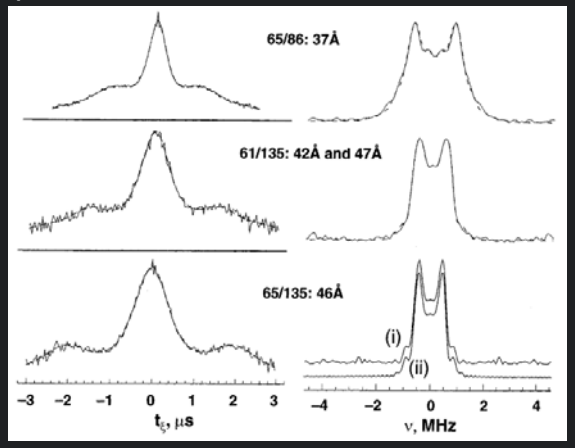

Left: Time evolution of DQC Signal from doubly labeled T4L; Right : their FT's

Table 3. Comparisons of Average Distances between Nitroxides, R_{av}, from the DQC Experiments (cf. Table 2) with the Distances, $R_{\alpha\alpha}$ and $R_{\beta\beta}$, between the Respective α- and β-Carbons, Obtained from X-ray Crystallography[60]

mutant	R_{av}, Å	$R_{\alpha\alpha}$, Å	$R_{\beta\beta}$, Å	Δ^a, Å
61/80	34, 29	28.7	28.82	5.3, 0
65/80	28.0[b]	22.6	22.4	5
65/76	21.4	16.7	16.6	4.7
61/86	37.5, 33.5	34.4	37	3, 0.9
65/86	37.4	28.86	31.17	8.5
61/135	47.2, 41.8	37.7	40.43	9.5, 4
65/135	46.3	34.26	36.67	12
80/135	36.8	26.7	27.4	10

[a] $\Delta \equiv R_{av} - R_{\alpha\alpha}$. [b] Average of distances from X- and Ku-bands.

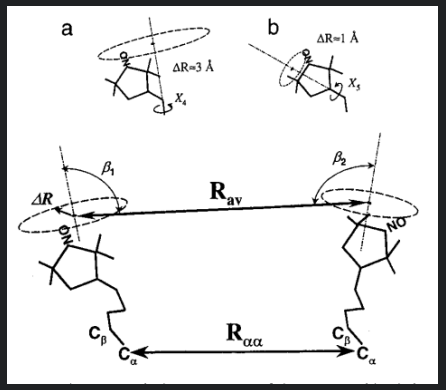

Accounting for Flexibility of Tether

DEER & DQC Pulse Sequences

DEER 4-pulse Sequence

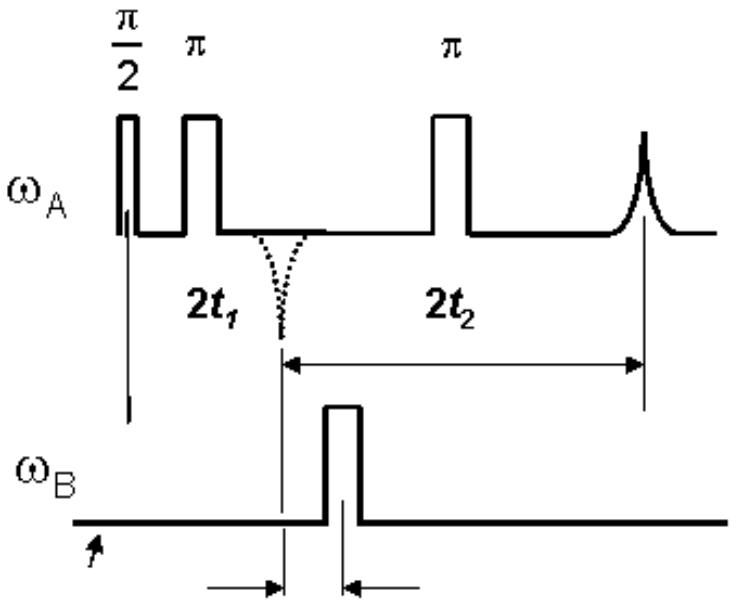

Signal amplitude $V = V_0[1 - p(1 - \cos \omega_d t_x)]$

Pump-probe technique irradiates only a fraction of spins with ca. 15-30 ns. pulses. (5-10G).

DQC 6-pulse Sequence

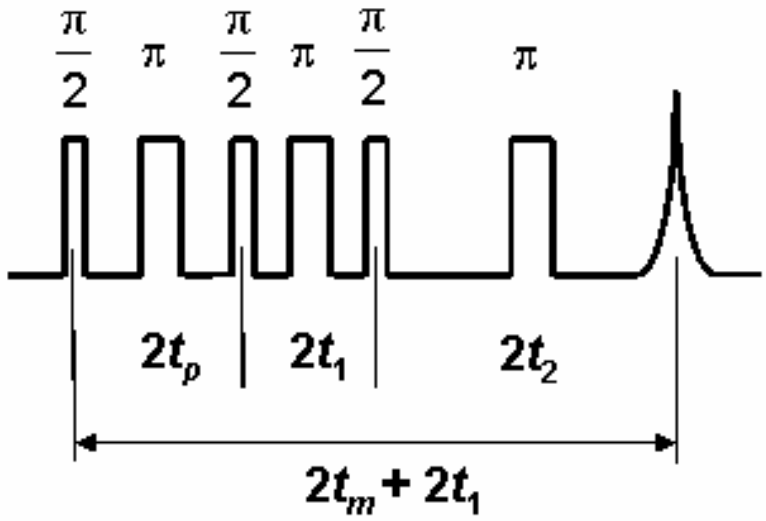

Signal amplitude

$$\omega_d = \frac{\gamma_e^2 \hbar}{r^3}$$

$$V = -\sin \omega_d t_p \sin \omega_d (t_m - t_p)$$
$$= \frac{1}{2}[\cos \omega_d t_m - \cos \omega_d t_\xi]$$

$$t_\xi = t_m - 2t_p$$

Irradiates (nearly) all the spins with 3 ns. pulses (30-60G).

Sensitivity Achievable: Depends on Several Factors

Pulse Sequences: 6 Pulse DQC

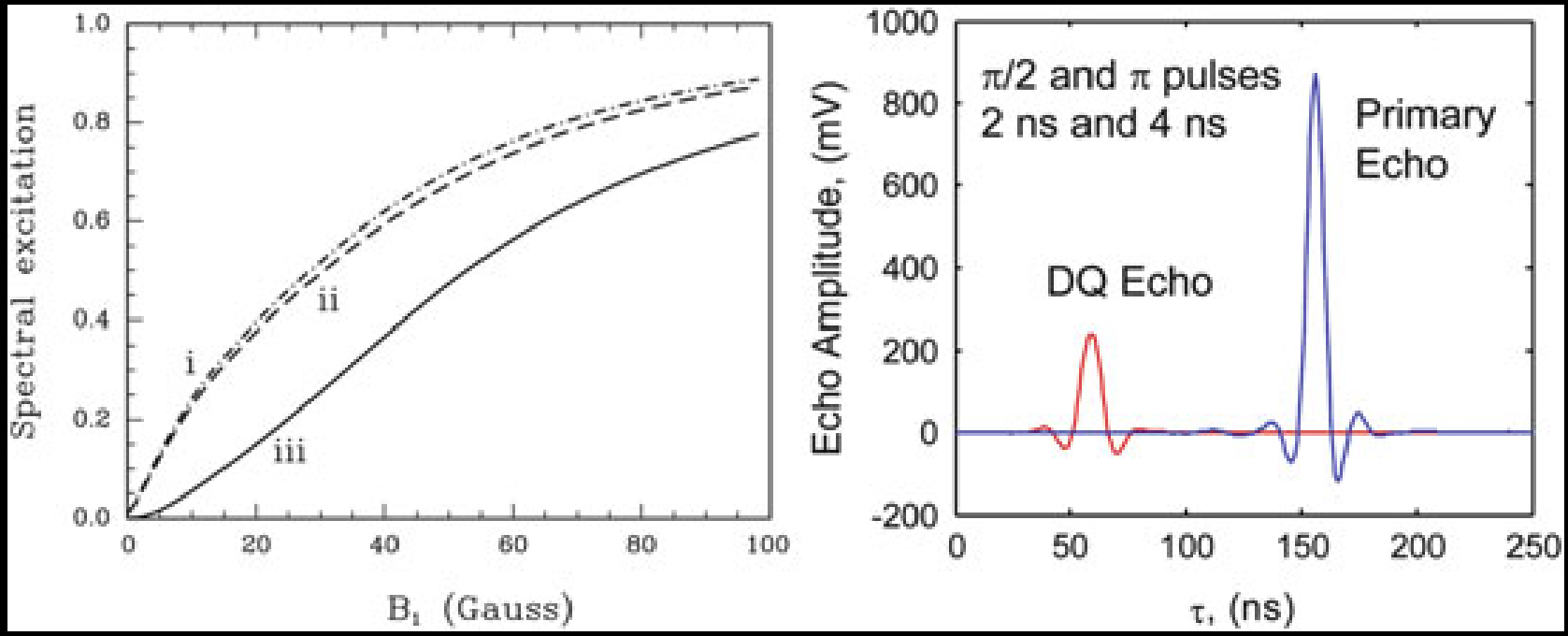

Signal Amplitude vs. B_1 (iii)

*Dipolar ESR: Distance Measurements, Borbat & Freed in Structure & Bonding, Springer, Berlin (2013). Web Link: http://link.springer.com/chapter/10.1007/430_2012_82

DQC-Echo is 26% of primary echo with $\pi/2$ & π pulses of 2 & 4 ns. resp. for B_1 = 45G,17.3GHz. (Theoretical Limit is 50% of primary echo)

Pulse Sequences: 4-Pulse DEER

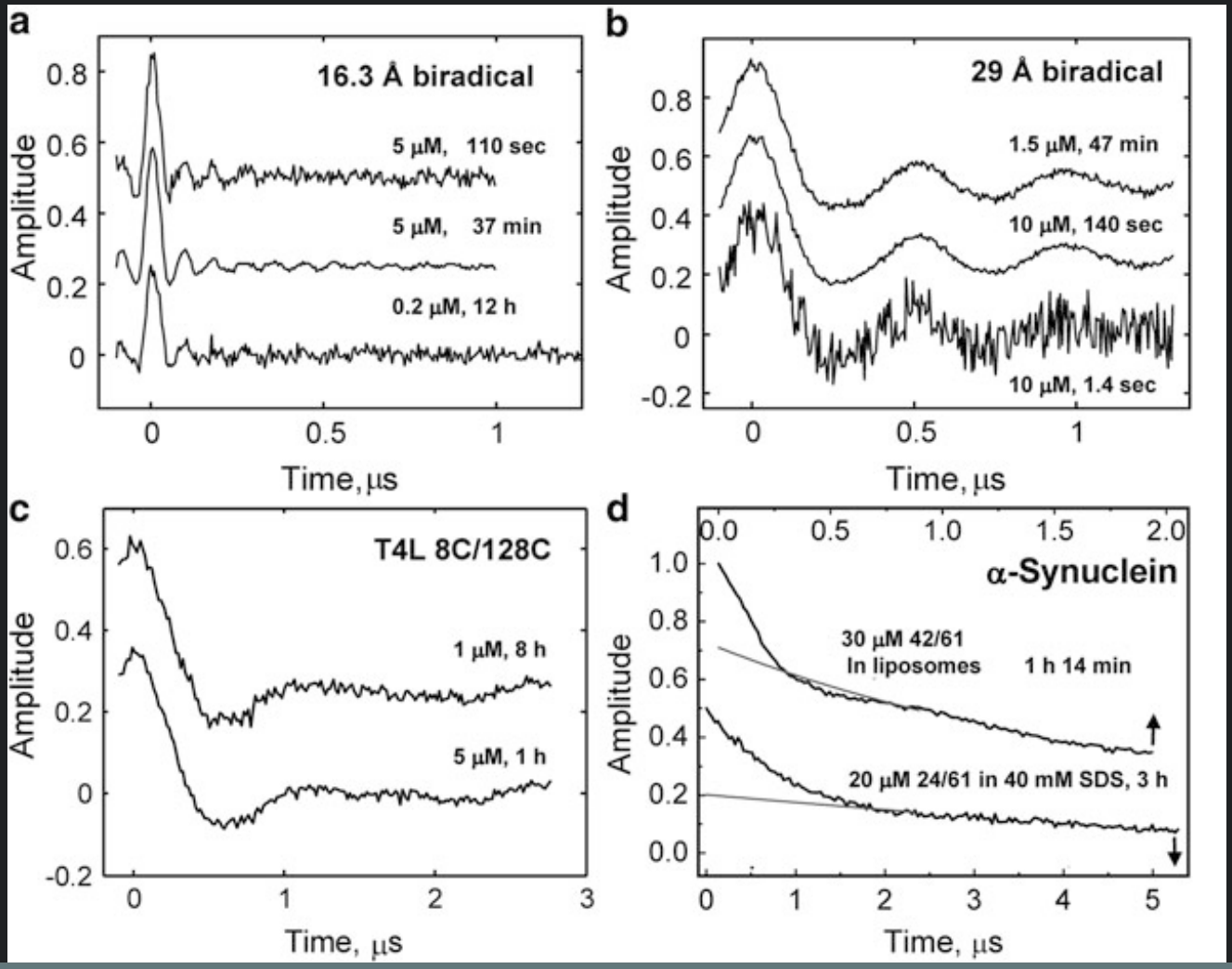

- Sensitivity of Ku-band (17.3 GHz) DEER
- Micromolar concentrations are readily studied.

***Borbat & Freed (Structure and Bonding)**

Pulse Sequences: Theory

SNR for PDS: Dependence on Frequency*

$$S_1 \propto \omega^2 C V_c^{\frac{1}{2}} \eta K B_1/B_s^2$$

S_1= Single Shot SNR of part of echo modified by dipolar coupling.

Let $V_c = \alpha\omega^{-3}$ **α fn. of resonator design.**

Concentration Sensitivity: $S_1(C) \propto \omega^{\frac{1}{2}} C \alpha^{\frac{1}{2}} \eta K B_1/B_s^2$

Absolute Spin Sensitivity: $S_1(N) \propto \omega^{\frac{7}{2}} N\alpha^{-\frac{1}{2}} K B_1/B_s^2$

For High Frequencies >ca. 90 GHz, then $\gamma B_s \propto \omega$

$$S_1(C) \propto \omega^{-\frac{1}{2}} C\alpha^{\frac{1}{2}} \eta K B_1/B_s$$

$$S_1(N) \propto \omega^{\frac{5}{2}} N \alpha^{-\frac{1}{2}} K B_1/B_s$$

Can B_1 "keep up" with B_s increase?

$$K = K' K_1^{\frac{1}{2}}$$

K´ depends on pulse method

$K_1 = Q\frac{\gamma B_1}{\omega}$ $K_1 \approx 0.1-0.2$ **for DEER**

≈ 1 **for DQC**

B_s = spectral extent in Gauss

$\eta = V_s/V_c$ **= filling factor of resonator**

* P.P. Borbat & J. H. Freed, EPR Newsletter, 17, 21, (2007); P.P. Borbat & J. H. Freed, Biological Magnetic Resonance, 19, 383, (2000).

New Technology: 5-Pulse DEER*

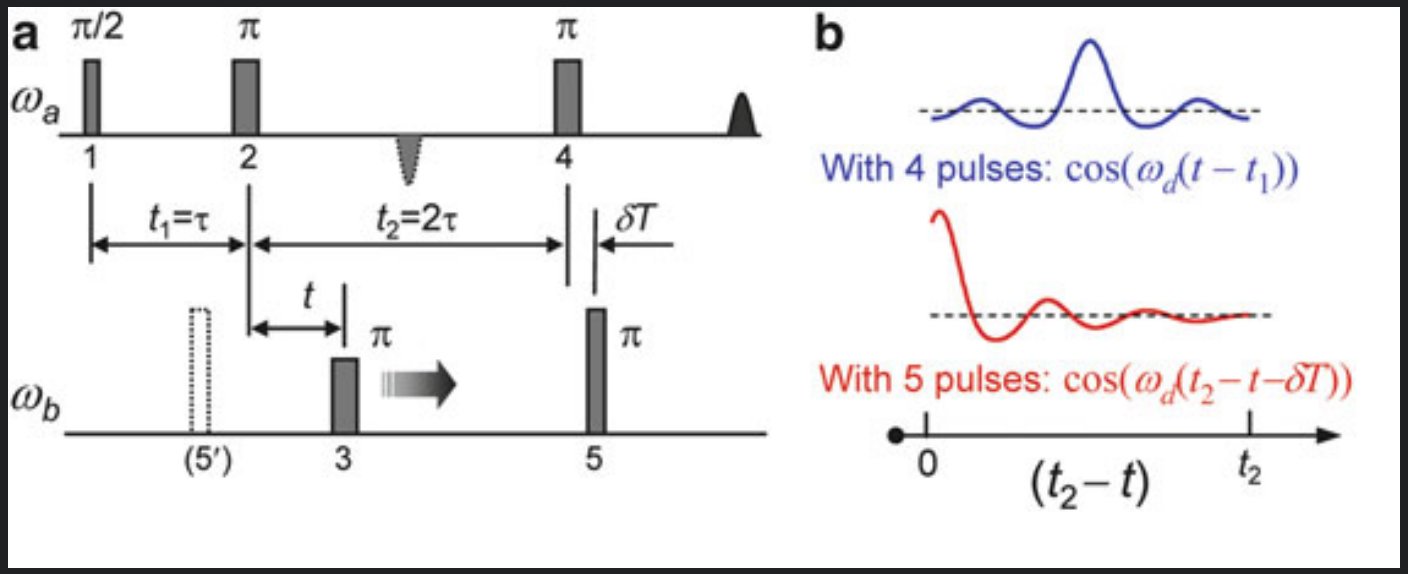

- Uses extra pulse: 5
- Proceeds as in 4-pulse DEER by stepping out t but $t_2 = 2\tau$ which minimizes phase relaxation due to nuclear spin diffusion from surrounding proton bath
- Pulse 5 enables using full evolution time

*** Borbat, Georgieva, Freed, JPC Letts. 4, 170 (2013)**

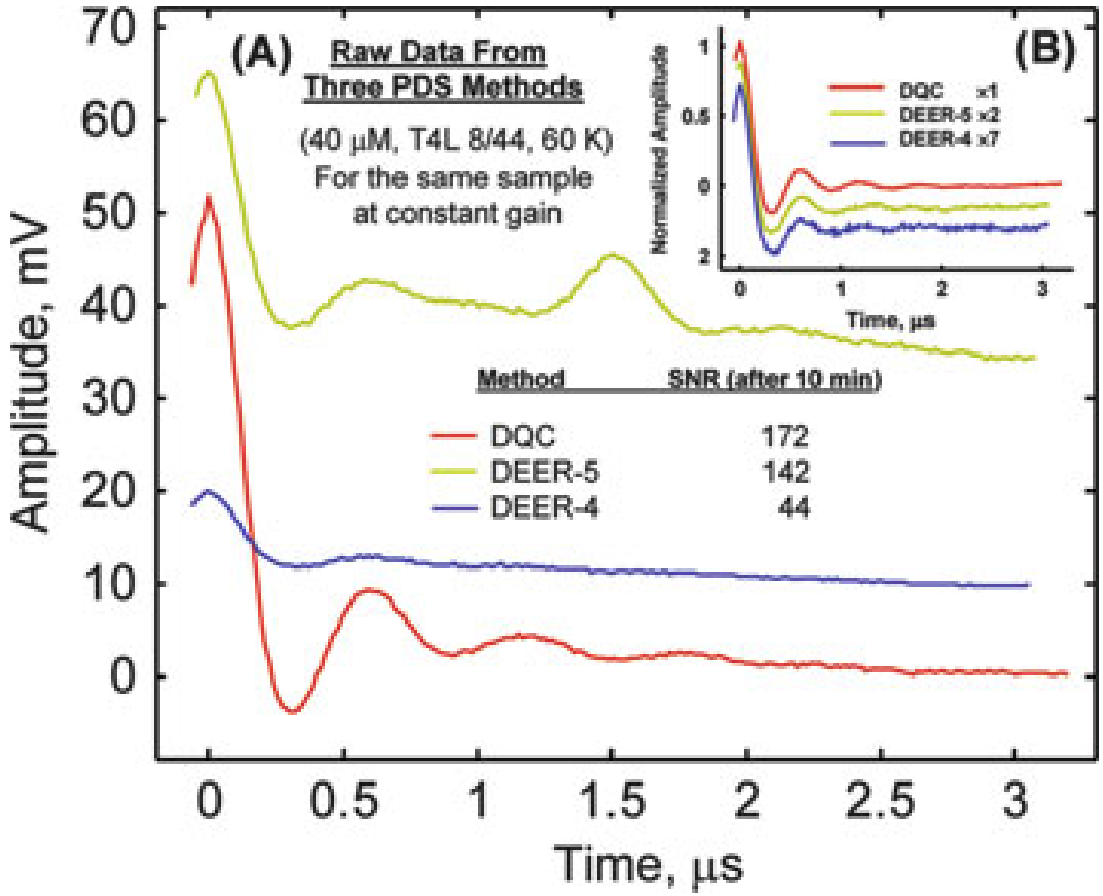

Sensitivity Comparison of DEER-4, DEER-5, & DQC-6

Borbat, Georgieva & Freed

Large Distances by Double-Quantum Filtered Refocused Electron Spin-Echoes

26 bp RNA structure with the nitroxide label that is attached to 4-thiouridine shown. Distance between them was measured to be 65 Å from the high-resolution X-ray crystal structure. We estimate the distance between spin labels to be 70 ± 5 Å.

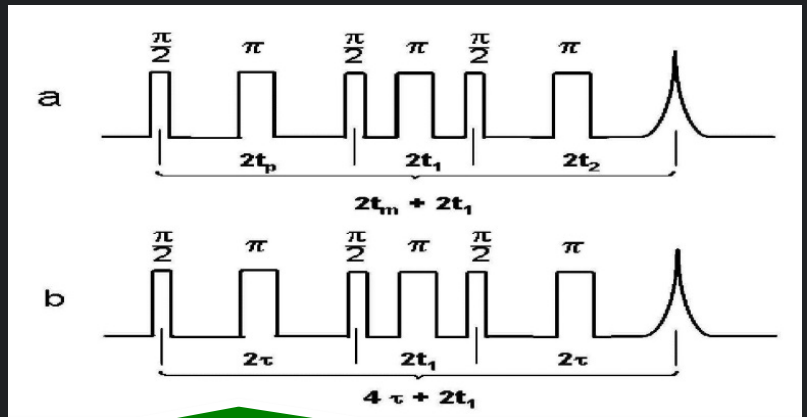

Six-pulse sequence used in (a) DQC ESR & (b) DQFR-ESE. In (b) one steps out 2τ & detects the refocused echo at 4τ + 2t1.

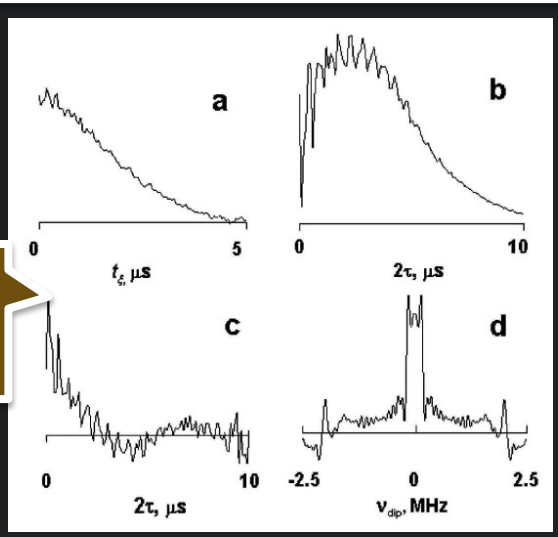

DQC ESR, (a) & DQFR-ESE (b) signal traces. DQFR-ESE signal (c) after removing relaxation decay & making standard linear baseline corrections & its Fourier transform (d)

Borbat, Davis, Butcher, Freed, JACS, 126, 7746 (2004)

The Challenge of Short Distances With the Example of Short Biradicals Used for DNP

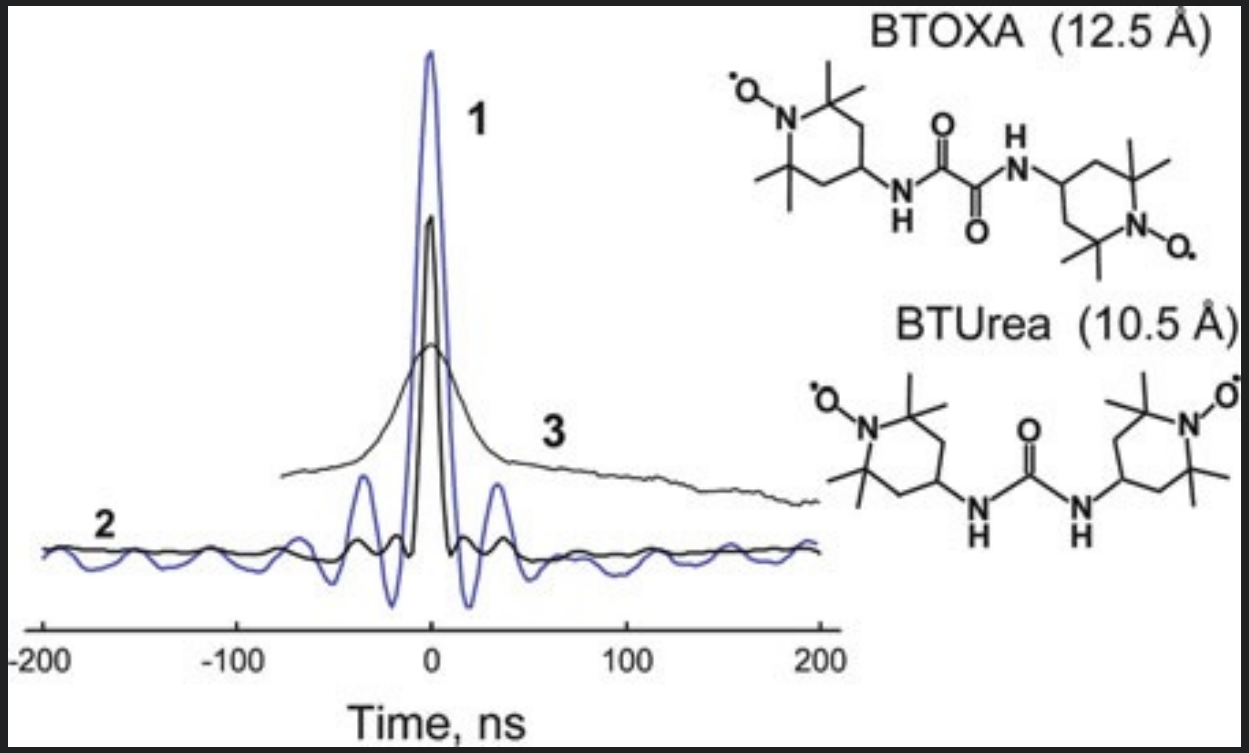

Kuband (17.3 GHz) DQC (1) & DEER (3) are compared for a rigid ~12.5 A° nitroxide biradical, BTOXA. Detection p/2 & p-pulses in 4-pulse DEER were 16 and 32 ns, respectively; the pumping pulse was 18 ns (B1 ~ 10 G).

This is found to be insufficient to properly excite the dipolar spectrum. (2)

Ku-band (17.3 GHz) DQC signal for an even shorter biradical, BTUrea.

Borbat & Freed (Structure and Bonding)

The Determination of Distance Distributions in PDS

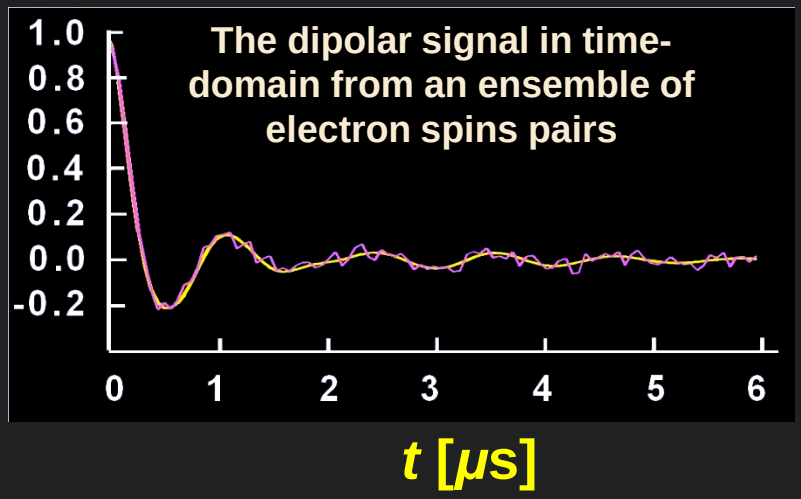

$$V(t) = \int_{R\,\min}^{R\,\max} K(r,t)P(r)dr$$

$$K(r,t) = \int_{0}^{1} \cos[(1-3x^2)\omega_d t]dx$$

$$\omega_d = \frac{\gamma_e^2 \hbar}{r^3} \quad , \quad x = \cos\theta$$

V(t) - the experimental time-domain signal from spin pairs.

P(r) - the distance distribution in pairs defined on the interval [R_{min} , R_{max}].

K(r,t) - the kernel for the Fredholm equation and can be of more complex form, if necessary

The Problem of Determination of Distance Distributions in PDS

A formal solution of the ill-posed Fredholm equation of the first kind by Singular Value Decomposition

$$P_\lambda = \sum_i \frac{u_i^T S_0}{\sigma_i} v_i$$

SNR~10^4

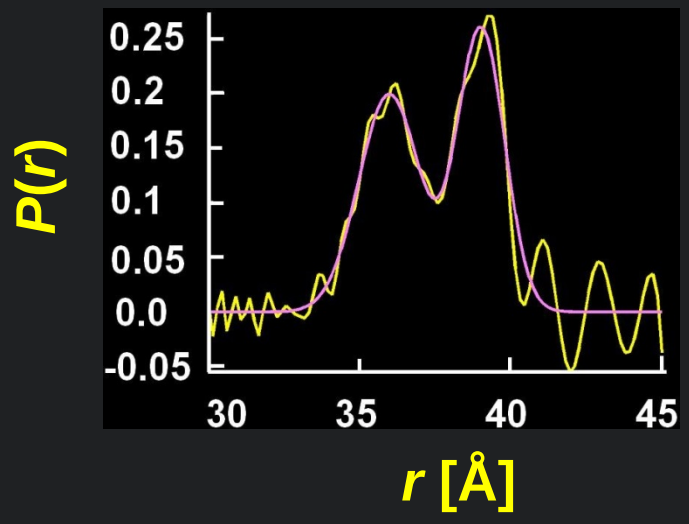

SNR~100

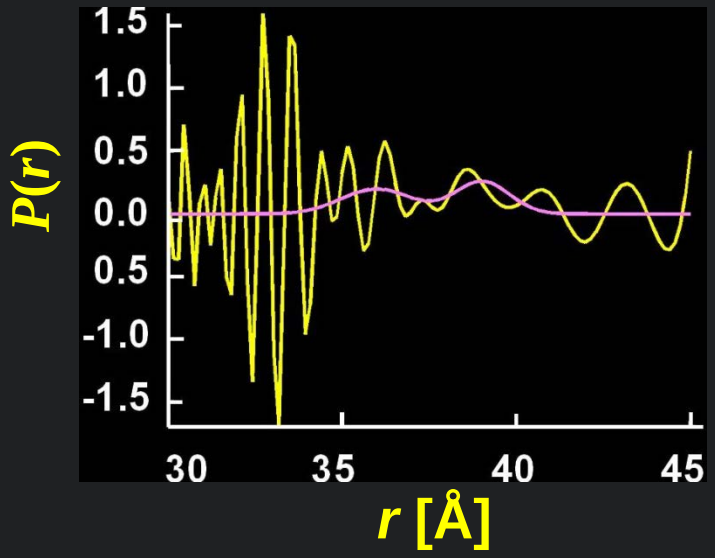

SVD fails to recover the original data due to the noise in *V*(*t*) and the effect of very small singular values .

Tikhonov Regularization: The L-curve Criterion

The regularization parameter λ is introduced to minimize the functional $\Phi[P]$

$$\Phi[P] = \|KP - S_0\|^2 + \lambda^2 \|P\|^2 \quad \Rightarrow \quad P_\lambda = \sum_i f_i \frac{u_i^T S_0}{\sigma_i} v_i \qquad f_i \equiv \frac{\sigma_i^2}{\sigma_i^2 + \lambda^2}$$

- **The quality of the result depends strongly on the regularization parameter λ.**
- **With a good λ, the second term leads to a smooth and stabilized estimate of the solution.**

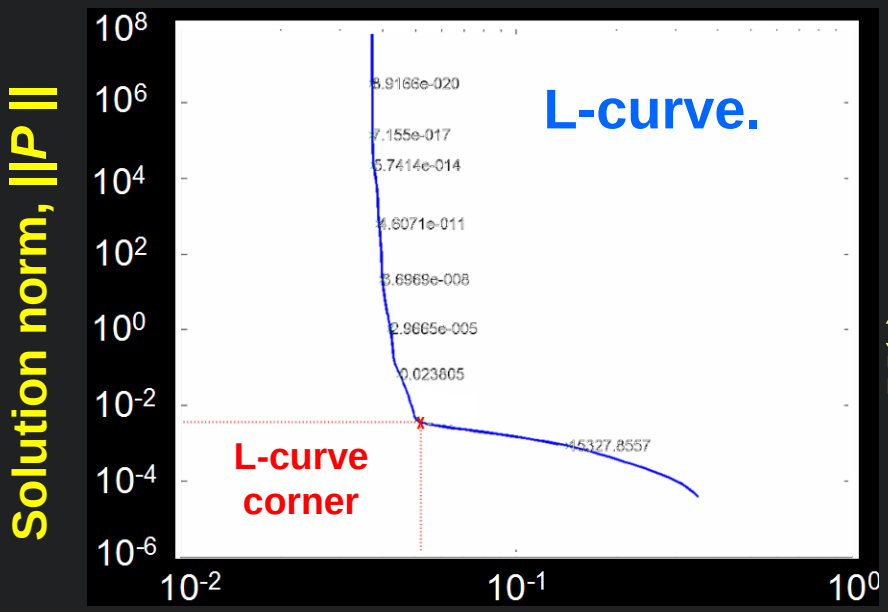

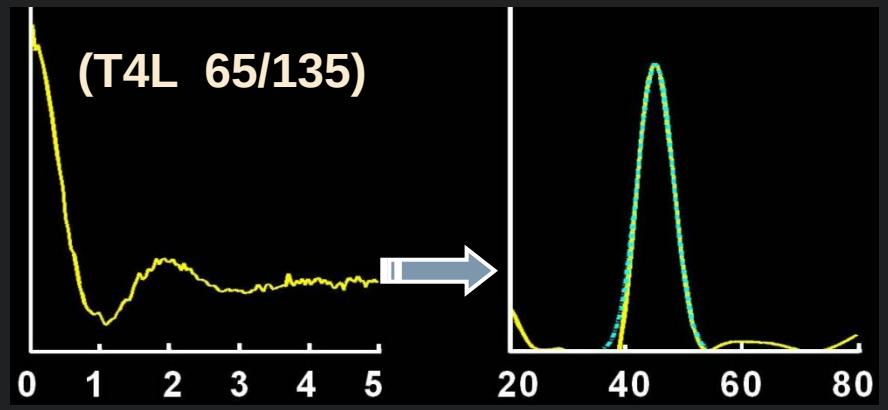

Chiang, Borbat, Freed, JMR 172, 279 (2005)

Maximum Entropy as a Tikhonov Regularization Refinement

Maximum entropy functional, $\Phi_{ME}[P]$

$$\Phi_{ME}[P] \equiv \|KP - S_0\|^2 - \lambda^2 E = \|KP(r) - S_0\|^2 + \lambda^2 \int P(r) \ln P(r) dr$$

⇒ *- infinity*

implicitly provides non-negativity constraint on $P(r)$

Modified functional:

$$\min\left\{ \|KP(r) - S_0\|^2 + \lambda^2 \int [P(r) \ln \frac{P(r)}{P_0(r)} + \frac{P_0(r)}{e}] dr \right\}$$

⇒ *zero*

MEM

1. **Is an iterative regularization based on Conjugate-gradients.**
2. **Requires good seed to avoid falling into local minima.**
3. **Is typically seeded with the L-curve solution.**
4. **Allows implementation of more complex schemes for processing of input data, e.g. to remove baseline.**

Chiang, Borbat, Freed JMR 177, 184 (2005)

Triangulation to Locate a Lipid at the Portal to the Lipoxygenase Active Site

B.J. Gaffney, M. Bradshaw, S. Frausto, J.H.Freed, P.P. Borbat, BJ, 103, 2134 (2012)

- Lipoxygenases are a family of enzymes of importance in development & in exerting control over first oxidative step in many unsaturated lipid signaling pathways.
- Lipoxygenase structures: devoted to shaping a curved substrate channel that approaches the centrally located active site iron ion.
- What is the site? Does the lipid enter with the polar end or methyl end first (i.e., head first or tail first)?
- We determined the location of a lipid spin in the protein structure by triangulation, or distance geometry.

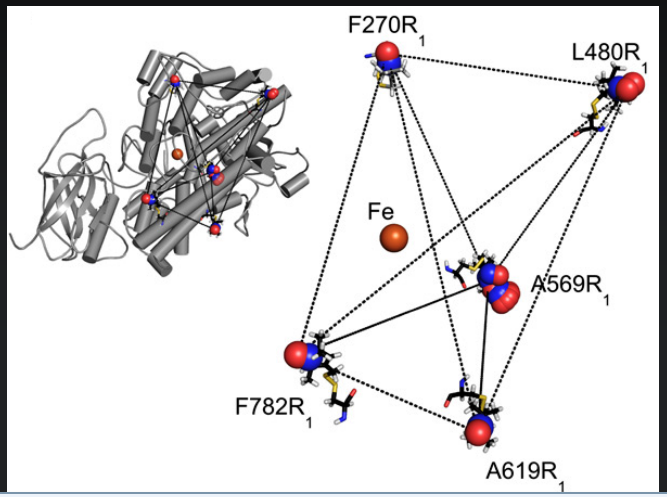

Experimental strategy: Placement of the spin-labeled R1 side chain, replacing natural side chains, in the structure of soybean seed lipoxygenase-1 (SBL1) (PDB:1YGE). The coordinates of spin-labeled residues were generated with the software PRONOX and the x-ray structure. The allowed solutions for nitroxide oxygen (red) and nitrogen (blue) are illustrated (spheres), and one full nitroxide at each site is rendered (sticks). The catalytic iron ion is indicated (orange).

(Left) Placement of the spin label sites in the overall SBL1 structure. (Right) The calculated spin locations are enlarged.

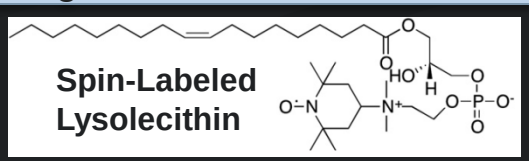

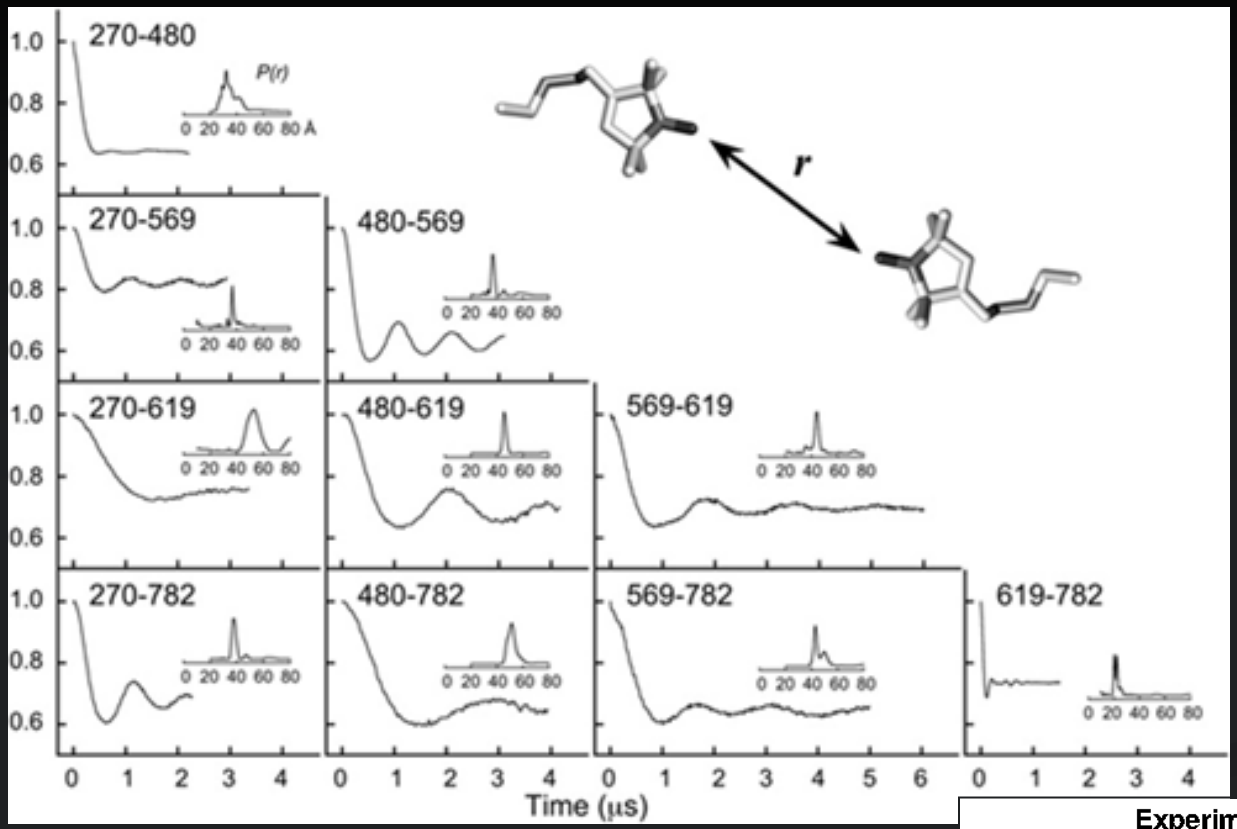

DEER/DQC Time Domain Data for the 10 Scaffold Distances in Lipoxygenase & Distance Distributions from them

Experimental pulsed (electron) dipolar spectroscopy (PDS) and calculated PRONOX distances in doubly spin-labeled soybean seed lipoxygenase-1 mutants

SDSL pair	PDS distance (Å)*	PRONOX distances (Å)†
270-480	32.5	30.1 ± 0.5
270-569	37	37.6, 39.5 ± 0.2, 40.3 ± 0.9
270-619	47	48.5
270-782	38	41.8
480-569	37.5	37.4 ± 0.1, 39.6 ± 0.4, 39.9 ± 0.5
480-619	46.5	46.0 ± 0.5
480-782	52.5	52.0 ± 0.7
569-619	44	39.7, 41.3 ± 1.4, 49.9 ± 0.8
569-782	44/52	47.3, 48.7 ± 0.7, 48.9 ± 1.1
619-782	20/22	22.0

***Experimental distances are the maxima in the distance distributions**

Distance Determinations From The LOPTC Spin To Spins On SBL1

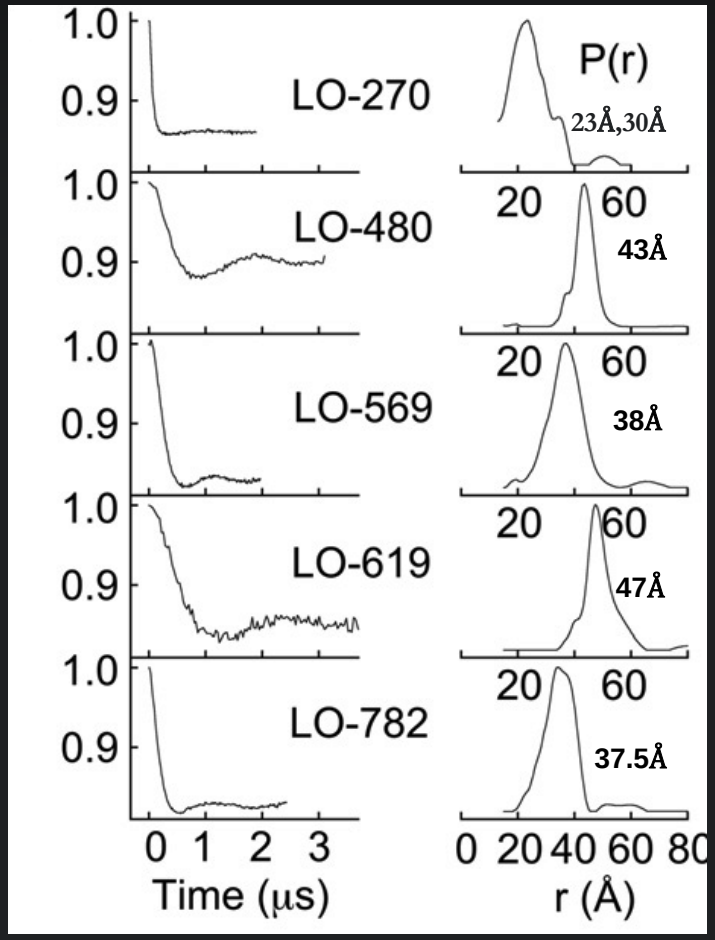

Used crystal structure of lipoxygenase SBL1 with PRONOX modeling & all 15 experimental distances were embedded in a Euclidian space by implementing metric-matrix distance geometry.

This approach could be employed to pinpoint the location and volume occupied by other flexible small molecules in a macromolecular complex.

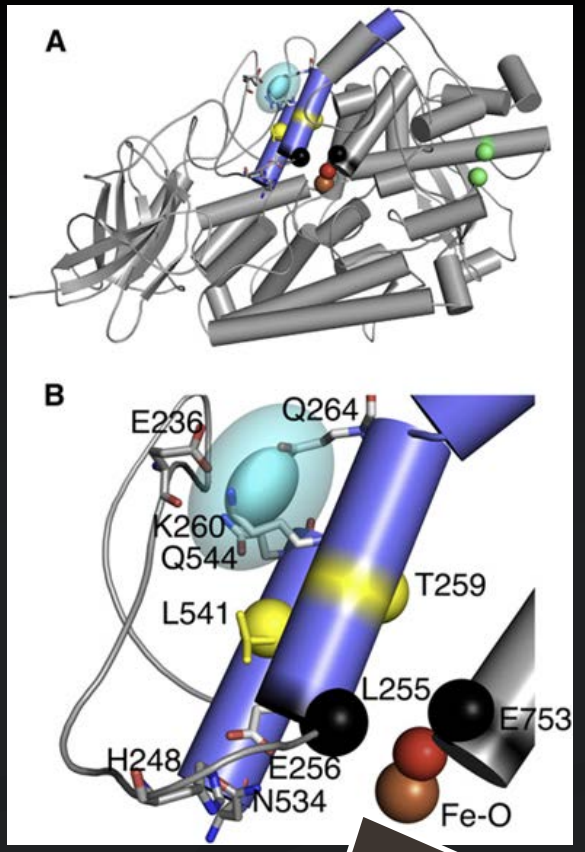

Experimental PDS solution for location of LOPTC spin superimposed on overall structure of SBL1

These PDS-ESR measurements placed the polar-end of LOPTC in a specific surface pocket (see fig. 6). The polar end inserts in a "head-first" manner. The 2σ envelope of the LOPTC spin location estimated to be <2Å, and exhibited some flexibility.

DQC-ESR of Gramicidin A: Membrane Channel Formation

Dzikovski, Borbat, Freed, BJ 87, 3504 (2004)

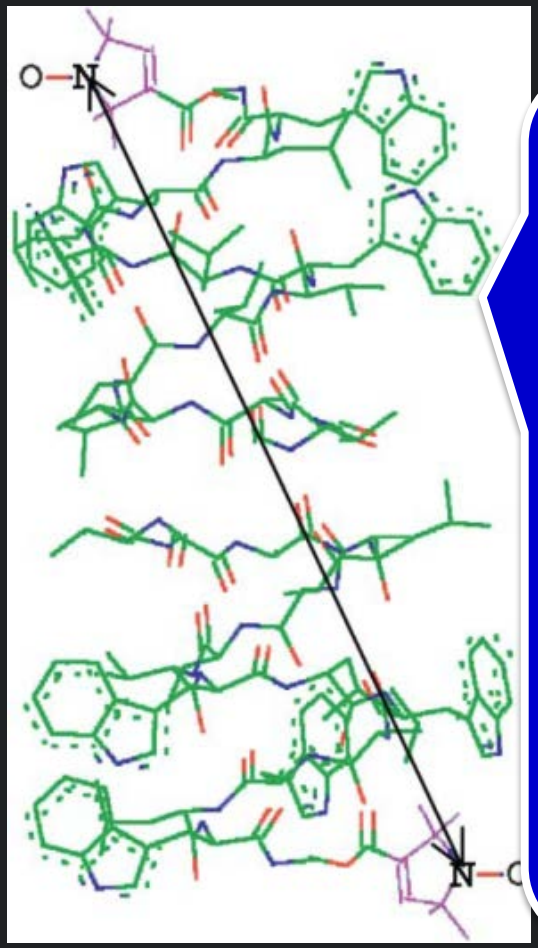

GAsI in the head-to-head conformation. The arrow indicates a distance of 29.5 A˚ between the nitroxide nitrogen atoms at the spin-labeling sites on the different C-termini of the dimer.

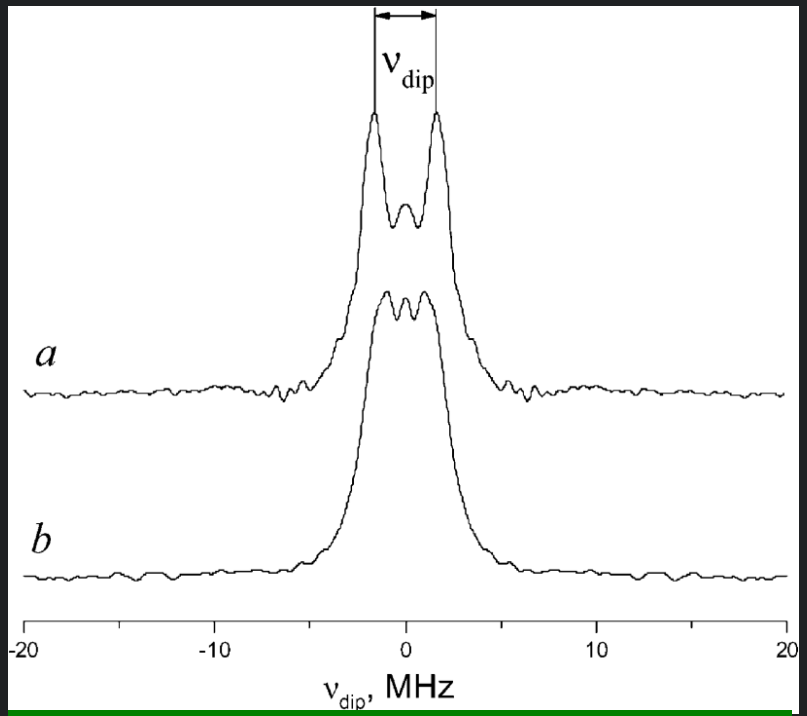

DQC-ESR spectra of GAsI dimers in (a) DMPC vesicles & (b) DPPC vesicles for a sample rapidly frozen to 77 K splitting corresponds to average distance of 30.9Å

Gramicidin Channels: Oriented Membranes and Dependence on Membrane Thickness

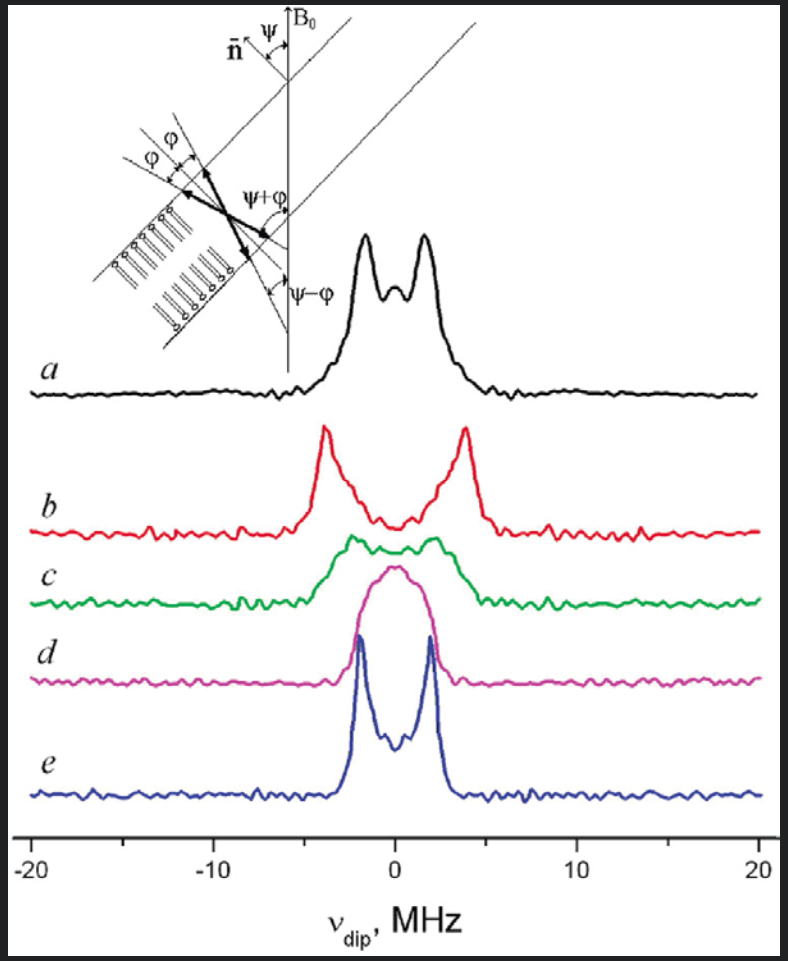

Pulse dipolar spectra of GASL in DMPC vesicles (a) & aligned DMPC membrane at different orientations of the magnetic field B_0 relative to the membrane normal nj : (b) ψ) 0°; (c) ψ) 30°; (d) ψ) 60°; (e) ψ) 90°.

Interspin Distances Measured for the GASL Channel Determined by Pulse ESR in Various Lipids

lipid environment	interspin distance, Å
GASL in DMPC membrane	30.9
GASL in DLPC membrane	28.8
GASL in didecanoyl PC membrane	28.6
GASL in DPPC membrane quenched after an exposure at 40 °C	31.4
GASL in DPPC membrane	no pairs detected
GASL in DSPC membrane	no pairs detected
GASL in DOPC membrane	28.7
GASL in POPC membrane	31.0
GASL in egg yolk lecithin	30.2

Dzikovski, Borbat, Freed, JPCB, 115, 176 (2011)

Functional Dynamics of ABC Transporters

Conformational Cycle of MsbA

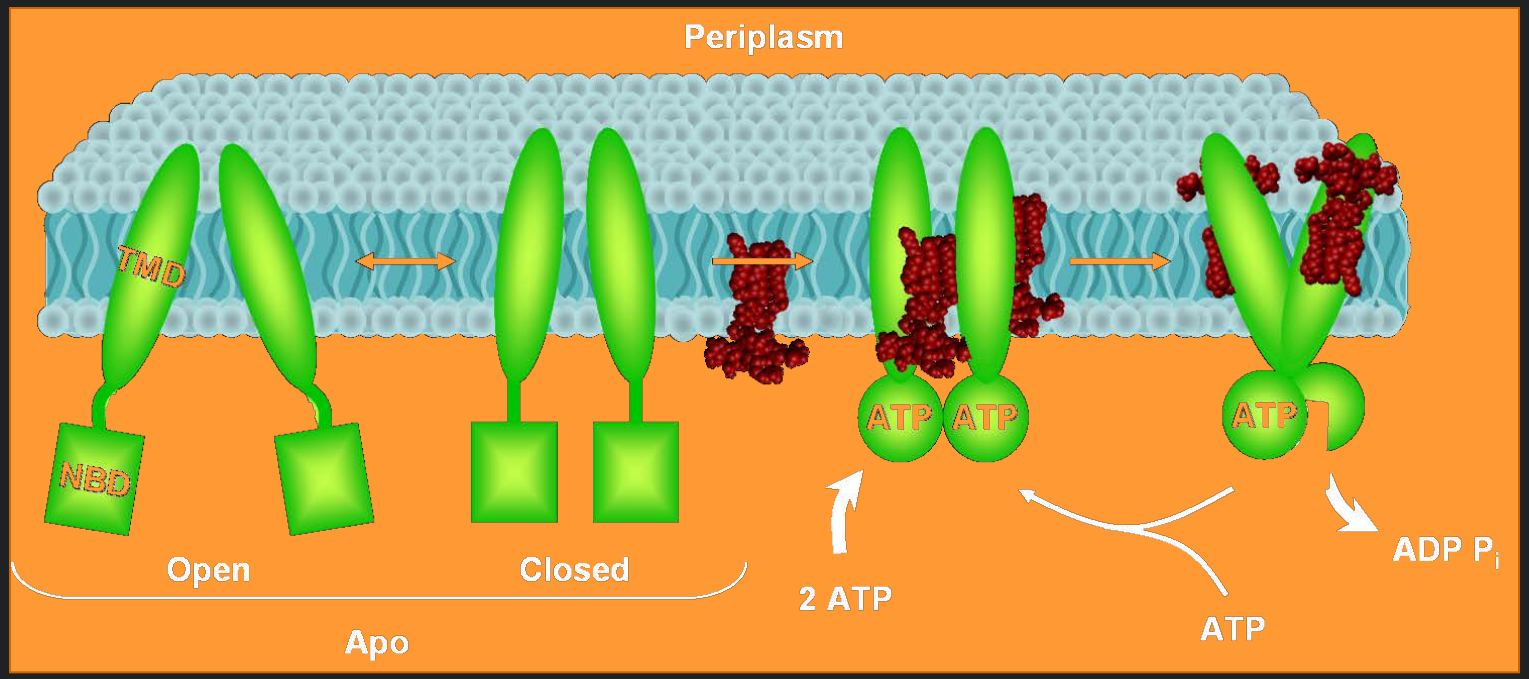

ABC transporters, such as MsbA, transport out of cells: cytotoxic drugs, structurally & chemically dissimilar molecules, against their concentration gradients. Energized by ATP hydrolysis, they act in a few power "strokes" culminating in drug expulsion.

The cartoon depicts flipping cytotoxic lipid (in brown) from the inner leaflet of the internal membrane of Gram-negative bacteria to the outer leaflet.

Dipolar Data & Distance Distributions for MsbA Reconstituted into Micelles & Liposomes

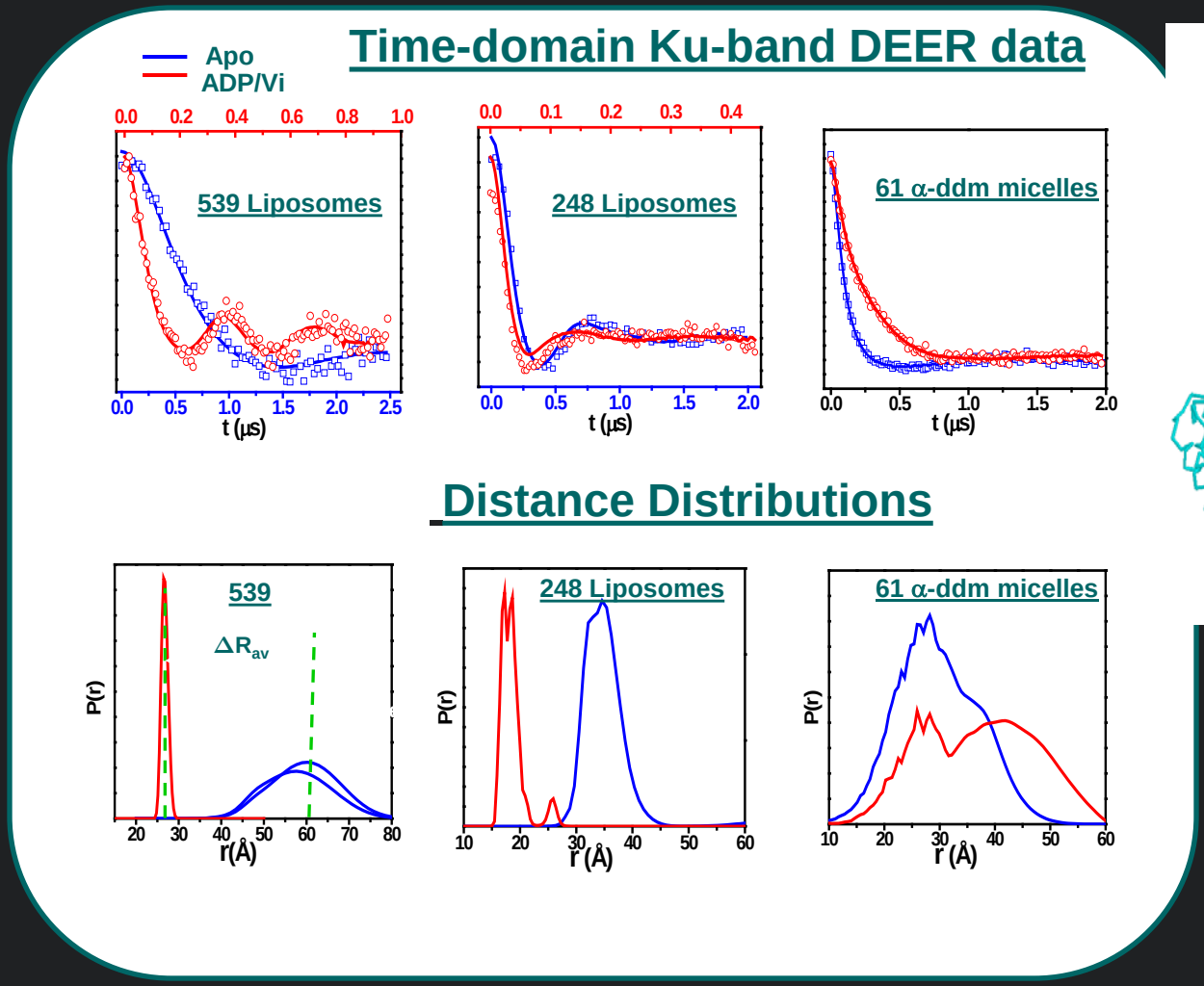

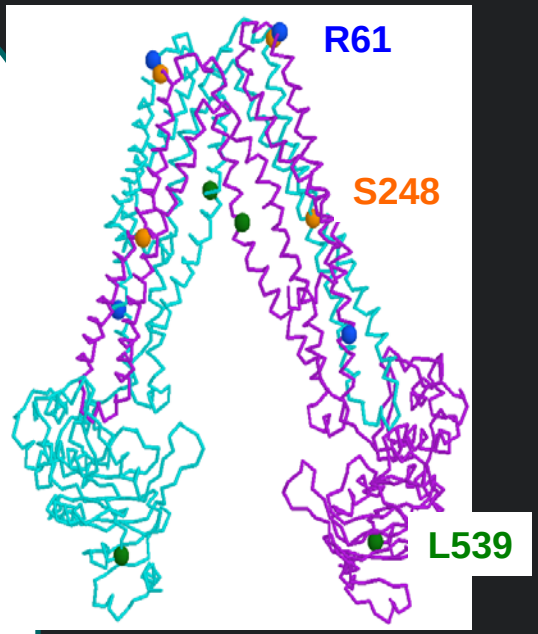

P.P. Borbat, K. Surendhran, M.Bortolus, P. Zou, J.H.Freed, H.S. Mchaourab PLoS Biology, 5, 2211, (2007)

2D-DQC: Orientations

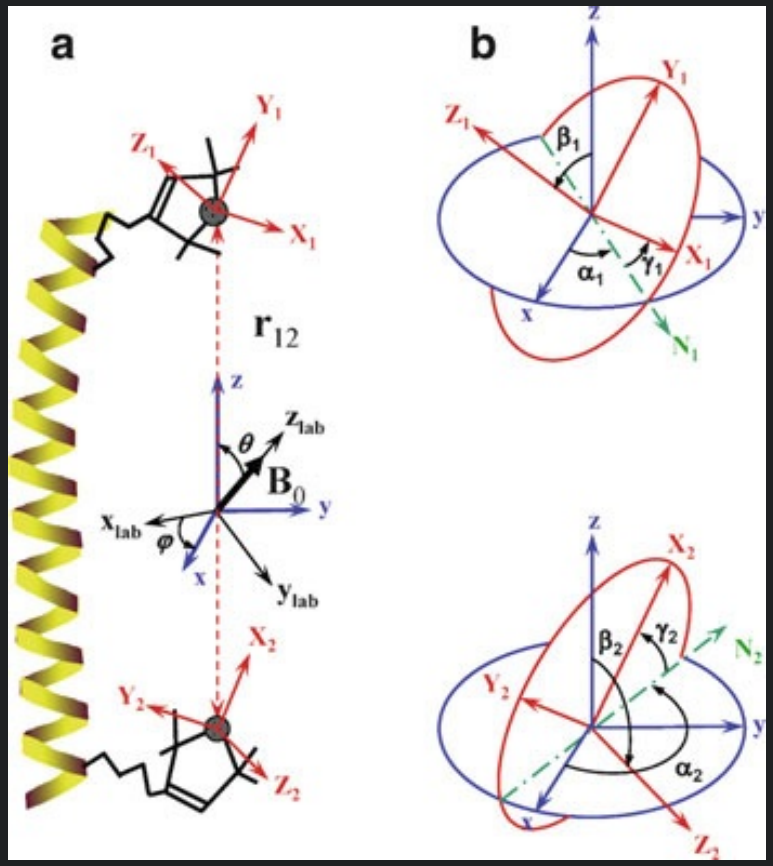

The set of Euler angles which define the orientations of the hf & g-tensor principal axes for nitroxides 1 & 2 in the dipolar (molecular) frame of reference

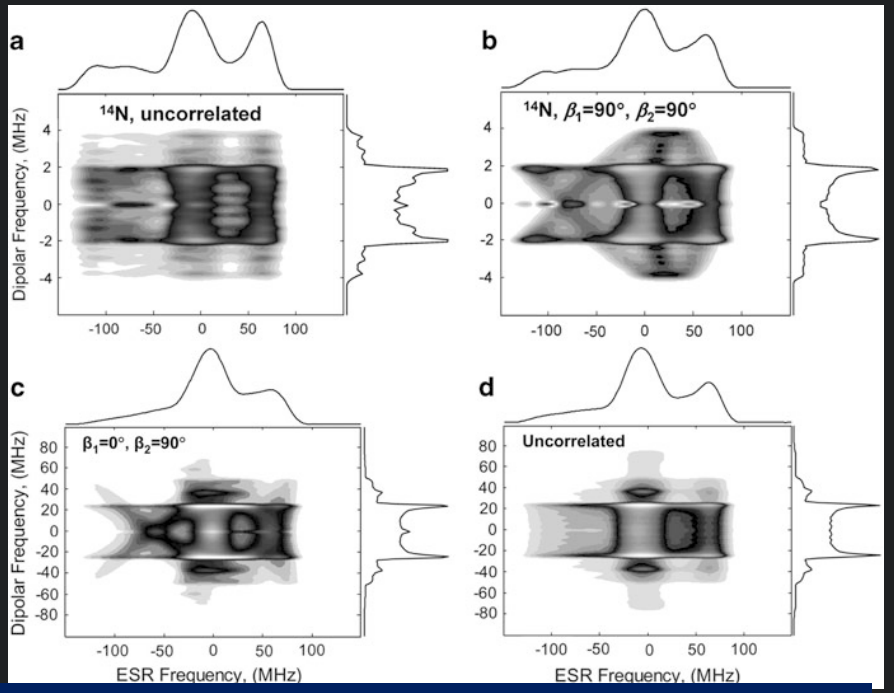

2D DQC magnitude filled contour plots obtained by 2D FT with respect to t_{dip} and t_{echo}. The magnitude 2D signal is summed along both dimensions & is shown as the 1D ESR absorption spectrum (at the top) or Pake doublet (on the rhs).
B_0=6,200 G., B_1=60G.
Top Row: r=29.6Å ($\upsilon_d = 2$MHz)
Bottom Row: r=12.7Å ($\upsilon_d = 25$MHz)

ACERT STAFF

Pëtr Borbat
Curt Dunnam
Boris Dzikovski
Keith Earle
Elka Georgieva
Kevin Hobbs
Alex Liqi Lai
Zhichun Liang
Jozef Moscicki
Joanne Trutko

Graduate Students:

Aritro Sinharoy
Dipanjan Samanta
Siddarth Chandrasenkaran

Previous:

Jaya Bhatnagar
Aharon Blank
Yun-Wei Chiang
Mingtao Ge
Wulf Höfbauer
Serguei Pachtchenko
Chang Shin
Andrew Smith
Dmitriy Tipikin
Ziwei Zhang

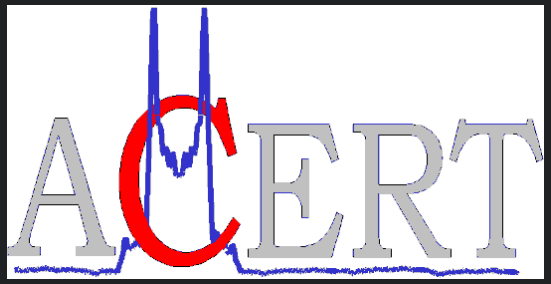

www.acert.cornell.edu

COLLABORATORS

Barbara Baird, Cornell Univ.
Olga Boudker, Weill-Cornell Medical
David Budil, Northeastern Univ.
Brian Crane, Cornell Univ.
Dale Edmondson, Emory Univ.
David Eliezer, Weill-Cornell Medical
Alberta Ferrarini, Univ. Padua
Mark Fleissner, UCLA
Betty Gaffney, Florida State Univ.
David Holowka, Cornell Univ
Wayne Hubbell, UCLA
Hassane Mchaourab, Vanderbilt Univ.
Charles Scholes, Univ. at Albany

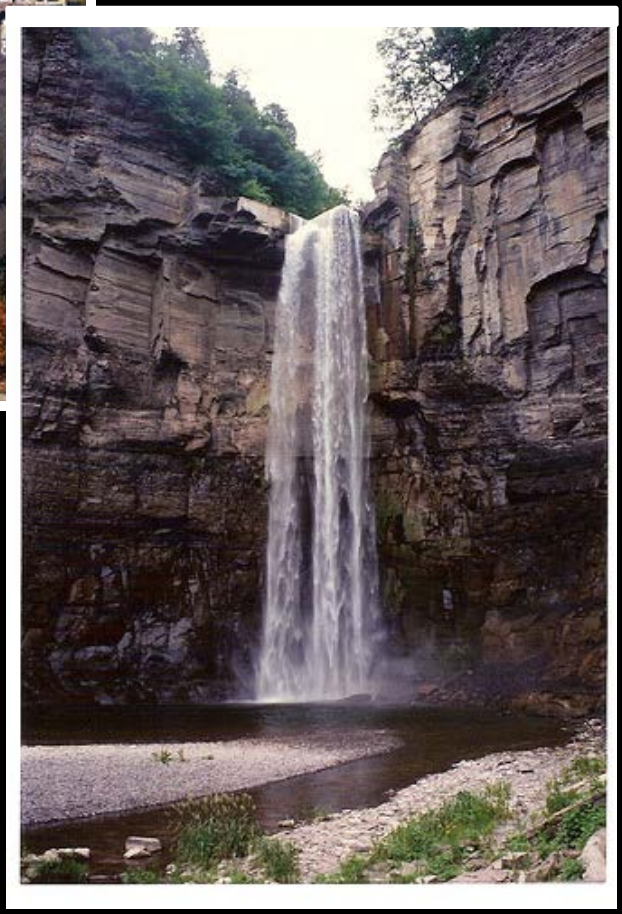

The End